JOURNAL OF MATERIALS SCIENCE 33 (1998) 173–182

Effect of methane concentration on physical properties of diamond-coated cemented carbide tool inserts obtained by hot-filament chemical vapour deposition

M. A. TAHER, W. F. SCHMIDT, H. A. NASEEM, W. D. BROWN, A. P. MALSHE
Materials and Manufacturing Research Laboratory, Mechanical Engineering Department–High Density Electronics Center HiDEC, University of Arkansas, Fayetteville, AR 72701, USA

S. NASRAZADANI,
Department of Materials Science, Iofahan Institute of Technology, Iofahan, Iran

Diamond-coated tools can greatly improve the productivity of machining highly abrasive materials such as high silicon–aluminium alloys used in the automotive industry. Cemented-carbide diamond-coated tool inserts have not become an off-the-shelf product owing to several difficulties including insufficient adhesion of diamond to the substrate and questionable reproducibilty in their machining performance in the manufacturing. In order to overcome these difficulties, a better understanding of the effects of the chemical vapour deposition (CVD) conditions such as methane concentration, reactor pressure and substrate temperature is important. In this work, cemented tungsten carbide tool inserts with 6 wt% Co (WC–Co) were coated with diamond films deposited at five different methane concentrations (1–9 vol %). Here we present *preliminary* results of the effect of methane concentration variation on the following physical properties of the diamond coating: surface morphology; crystal structure; chemical quality; surface roughness; residual stress. The results indicate that the best physical properties of diamond-coated tool inserts using hot-filament CVD are achieved with diamond coatings deposited at methane concentrations ranging from 1 to 3%.

1. Introduction

Diamond is a unique material for tooling applications because of its high Vickers hardness (10000 HV), high compressive strength (greater than 110 GPa) and high thermal shock resistance (greater than 1000 ΔT (K)), together with a low dynamic coefficient of friction (0.03) [1]. Owing to recent advances, it is possible to apply diamond coatings to cemented carbide and silicon nitride tool inserts [2–14]. Unlike diamond high-pressure obtained by high-temperature physical vapour deposition, chemical vapour deposition (CVD) thin-film coating technology allows the deposition of diamond films on complex geometries in a relatively cost-effective manner and, hence, there is increasing interest in its application for cutting inserts.

Numerous studies examining the effects of the CVD conditions on diamond film properties deposited on silicon [15–18] and thin pure tungsten substrates [19, 20] have been reported. No systematic studies were found in the *published* literature that address the effects of deposition conditions on diamond coatings deposited on state-of-the-art cemented carbide tools. Such an investigative study would provide the optimal set of conditions that results in a good-quality coated tool insert.

Film quality is a subjective term and depends on the type of application. In the case of tool inserts used for machining, the required diamond coating should have a desired graphitic content with well-faceted crystals, good adhesion with the substrate, uniform coverage over flank and rake regions, and uniform grain size. All have to be achieved at an acceptable growth rate. In practice, however, to obtain specific results, compromises have to be made in the choice of deposition parameters through an optimization process.

All deposition parameters such as the reactor pressure, the gas flow rates, the substrate surface temperature and the hydrocarbon gas percentage are interdependent. Therefore, for the reactor used in this work, an optimization process was undertaken to achieve an optimal thermal configuration at a fixed pressure, gas flow rate and methane concentration. Details of the thermal optimization process have been described elsewhere [21].

In this paper, the focus of the work is to examine several diamond coatings on WC–Co tool inserts

0022–2461

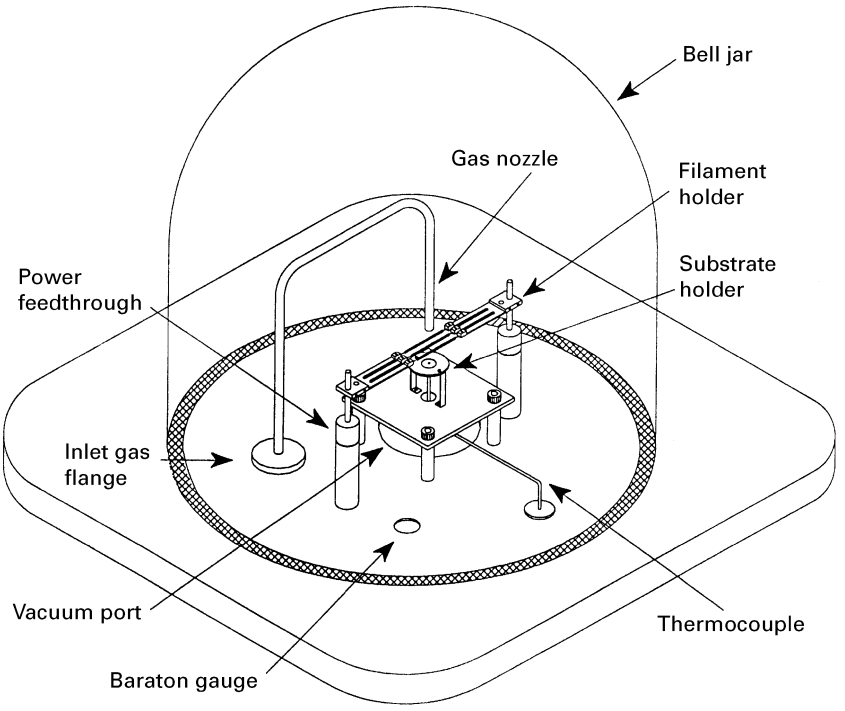

Figure 1 Layout of the HFCVD reactor.

deposited at various methane concentrations. The goal is to determine the optimal value of methane concentration for achieving a good-quality cutting tool.

2. Experimental procedure

Cemented carbide inserts style TPU 322, supplied by Rogers Tool Works were used as the substrate material. A proprietary pre-treatment technique was used on the inserts to enhance diamond deposition and adhesion. The reactor used for diamond deposition was a low-cost hot-filament CVD reactor shown in Fig. 1 having a tungsten wire of 0.3 mm diameter at a distance of 1 cm above the substrate. The reactor pressure was 2.66 kPa (20 Torr) and the total gas flow rate was 100 sccm. Selected values of methane concentration were 1, 3, 5, 7 and 9 vol %. The filament temperature was 2200 °C and was recorded using an optical pyrometer. The substrate temperature was 850 °C and was measured using a type K thermocouple. Using a deposition time of 20 h the film thickness of the deposited diamond films was 15 ± 3 μm and was measured by fracturing the surface using a Rockwell macrohardness tester.

The surface morphology was examined using a scanning electron microscope (Hitachi S-2300) with a maximum resolution of 45 nm and 25 keV maximum electron voltage. An X-ray diffractometer (Phillips Xpert system) was used to determine the crystal structure and to calculate the residual stress induced in the diamond coatings using the $d \sin^2 \Psi$ method. Detailed information of measuring the residual stress has been described elsewhere [22]. The X-ray system has a PW3710 diffractometer control unit which controls two goniometers. The source is a sealed Cu anode tube with a Kα wavelength $\lambda = 1.540\,60$ Å.

An ISA U-1000 macro-Raman spectrometer was used for chemical quality evaluation by Raman characterization. The instrument utilizes a 100 mW argon laser operating at the 514.5 nm line. The analysed area was a spot of 0.5 mm diameter on the cutting tip of the diamond-coated insert.

A Digital Instruments Nanoscope SPM atomic force microscope was used to measure the surface roughness of the diamond coatings on tool inserts.

3. Results and discussion

3.1. Surface morphology

The results of surface morphology analysis conducted by scanning electron microscopy on the five samples with various methane concentrations are shown in Fig. 2. The increase in methane concentration resulted in two variations. The first was at 3 vol % methane where the (100) orientation became dominant at the surface instead of the mixed (111) and (100) orientations exhibited at 1 vol % methane. Further methane increase beyond 3 vol % resulted in the formation of fine-grained diamond with cauliflower-like microcrystalline facets.

3.2. Surface defects and non-uniform morphology

Defects in the diamond film surface, such as localized growth, can occur as a result of improper cleaning of the substrate surface prior to deposition. Some surface defects were observed in this work as shown in Fig. 3. The defects were caused by the progressive growth of CVD diamond on a single diamond seed particle. This diamond particle was a residue from the polishing compound used to scratch the substrate surface. The defect had a unique flower shape consisting of several diamond crystals originating from the centre.

Non-uniform heat distribution can result in a non-uniform surface morphology of the diamond film. For

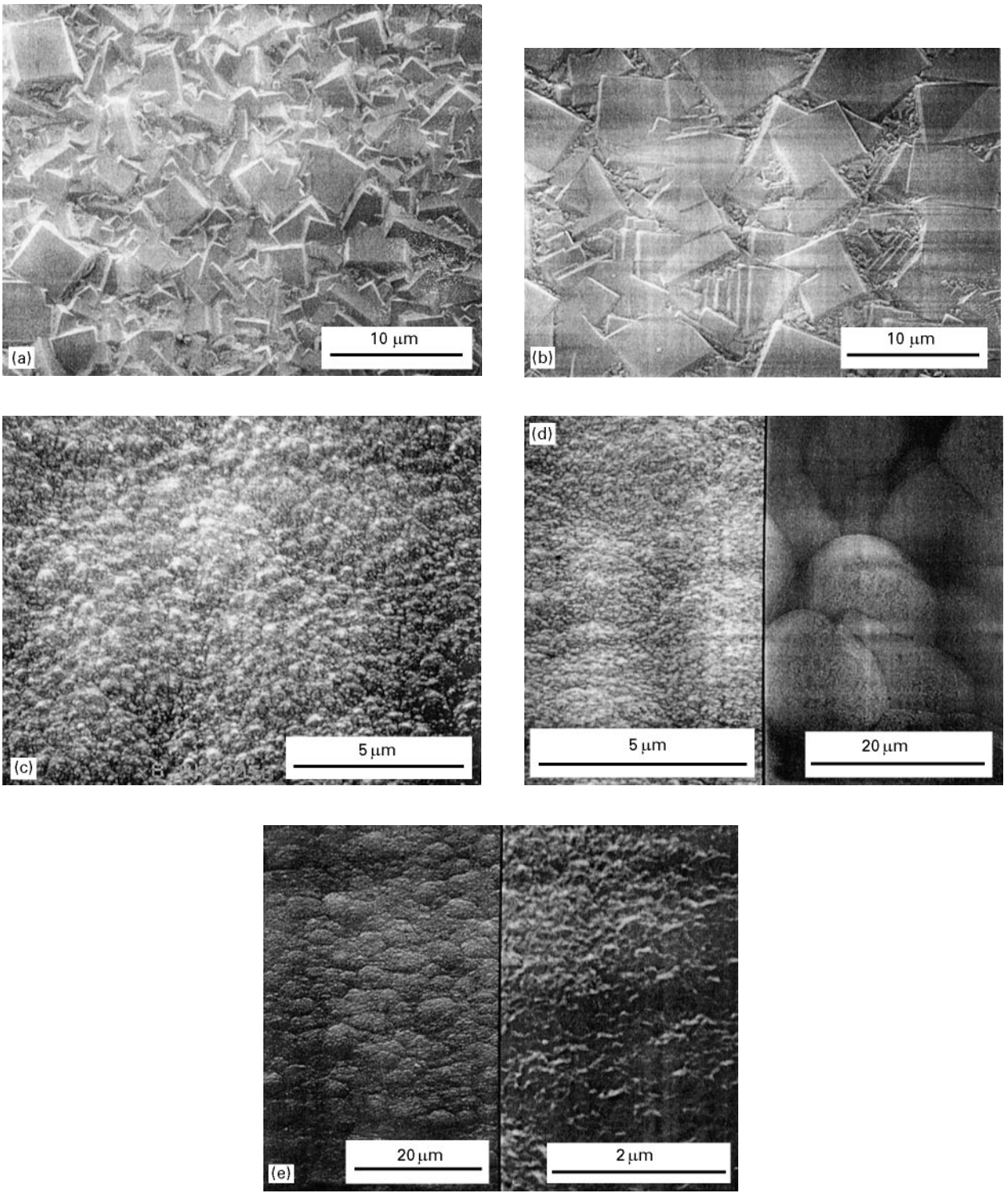

Figure 2 SEM photographs showing the surface morphologies of diamond coatings deposited at (a) 1, (b) 3, (c) 5, (d) 7, (e) 9 vol % methane, respectively.

example, samples with high methane concentrations (7 and 9 vol %) had a general non-faceted surface morphology. However, at areas very close to the filament, some highly twinned faceted crystals appeared as shown in Fig. 4. This shows that the morphology of CVD- grown diamond coatings on tool inserts can be affected by both the methane percentage and the substrate temperature distribution.

3.3. Cutting edge morphology

The critical region where the nature of the morphology is most important is at the cutting edge of a tool insert. The morphology must have minimum defects, and the diamond facets should be, as much as possible, aligned with respect to the cutting edge. Because the surface texture for the 3 vol % methane sample had a (100) orientation, a very-well-defined cutting edge was observed with a low average surface roughness ($R_a = 200.34\ \mu m$ measured by atomic force microscopy (AFM) as shown in Fig. 5a. Comparison of this morphology with that of a (111)-oriented film shows that the latter has a more rugged surface ($R_a = 388.44\ \mu m$ measured by (AFM) and a poorly defined cutting edge as shown in Fig. 5b. Increasing

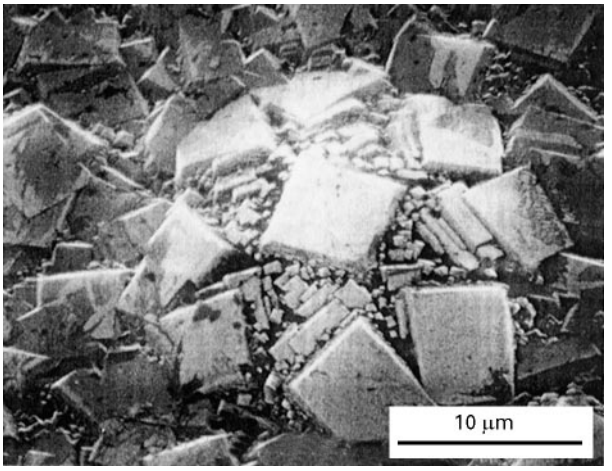

Figure 3 SEM photograph showing a flower-shaped surface defect in a diamond film deposited at 3% methane.

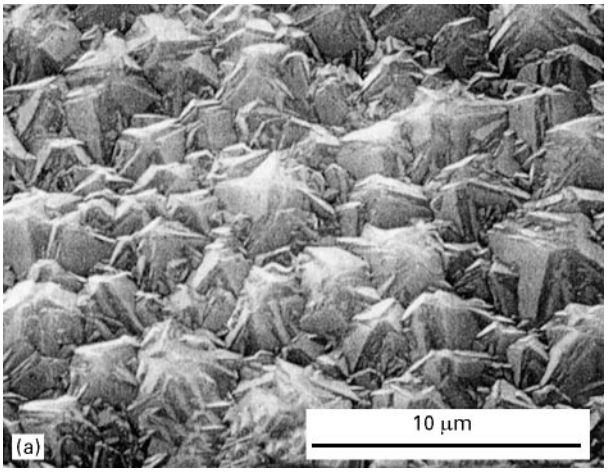

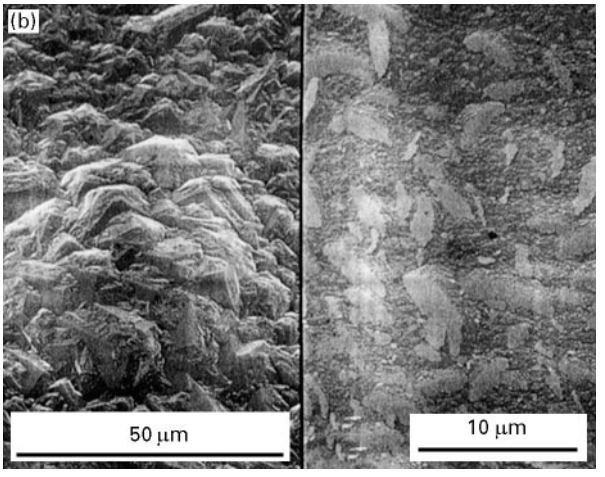

Figure 4 (a) Surface morphology of a diamond film with 5 vol % methane at area close to filament, (b) Surface morphology of a diamond film with 7 vol % methane at are close to filament. The right hand side portion of the photograph shows the transformation zone from a well-faceted morphology to a non-faceted one.

the methane concentration resulted in a smooth cutting edge morphology where the diamond crystals were ball-like shaped. The average surface roughness observed at 5–9 vol % methane had a value of 68 μm. The geometry of the cutting edge was well defined. However, as shown in Fig. 5c, some flaws appeared in the

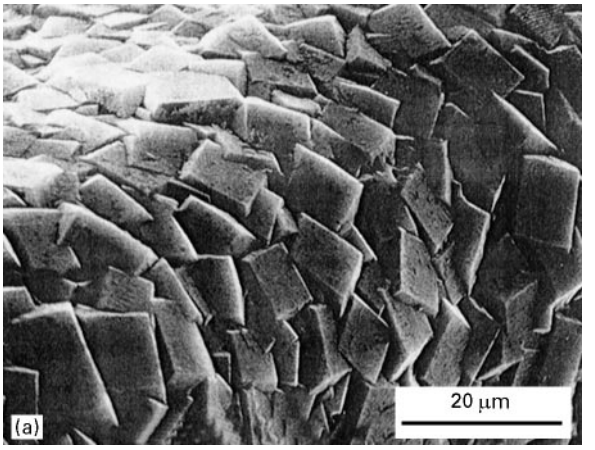

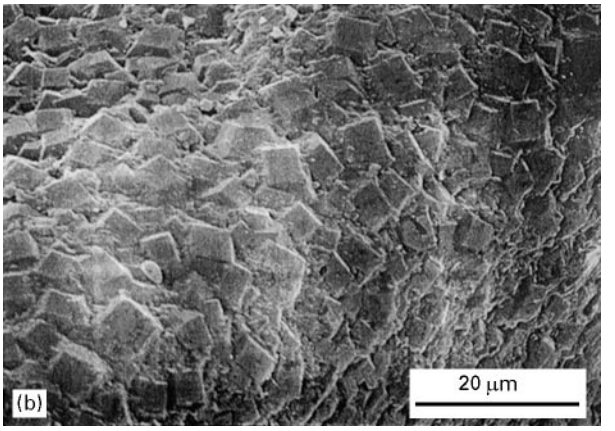

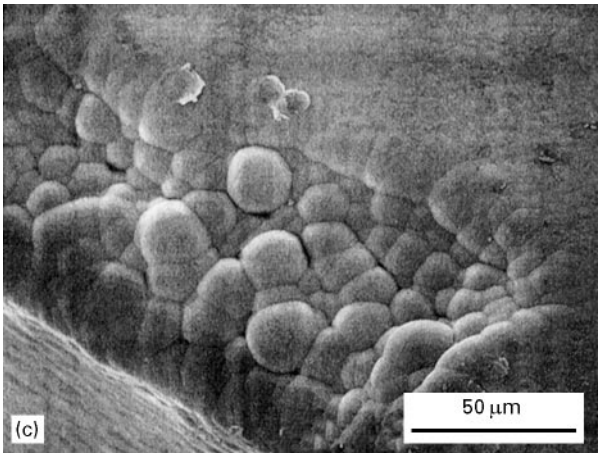

Figure 5 (a) Cutting edge morphology of a (100) oriented diamond film deposited at 3 vol % methane. (b) Cutting edge morphology of a (111) oriented diamond film with 1 vol % methane. (c) Cutting edge morphology of a diamond film with 7 vol % methane.

form of chipped regions that might have been caused by poor adhesion. The increased presence of methane resulted in an increased presence of non-diamond carbon species in between the diamond grains. These non-diamond species have loose and weak bonds, resulting in poor granular adhesion.

3.4. Crystal structure and texture

X-ray diffraction (XRD) spectra of the five diamond-coated samples deposited at various methane percentages are shown in Fig. 6. The ratios of the relative

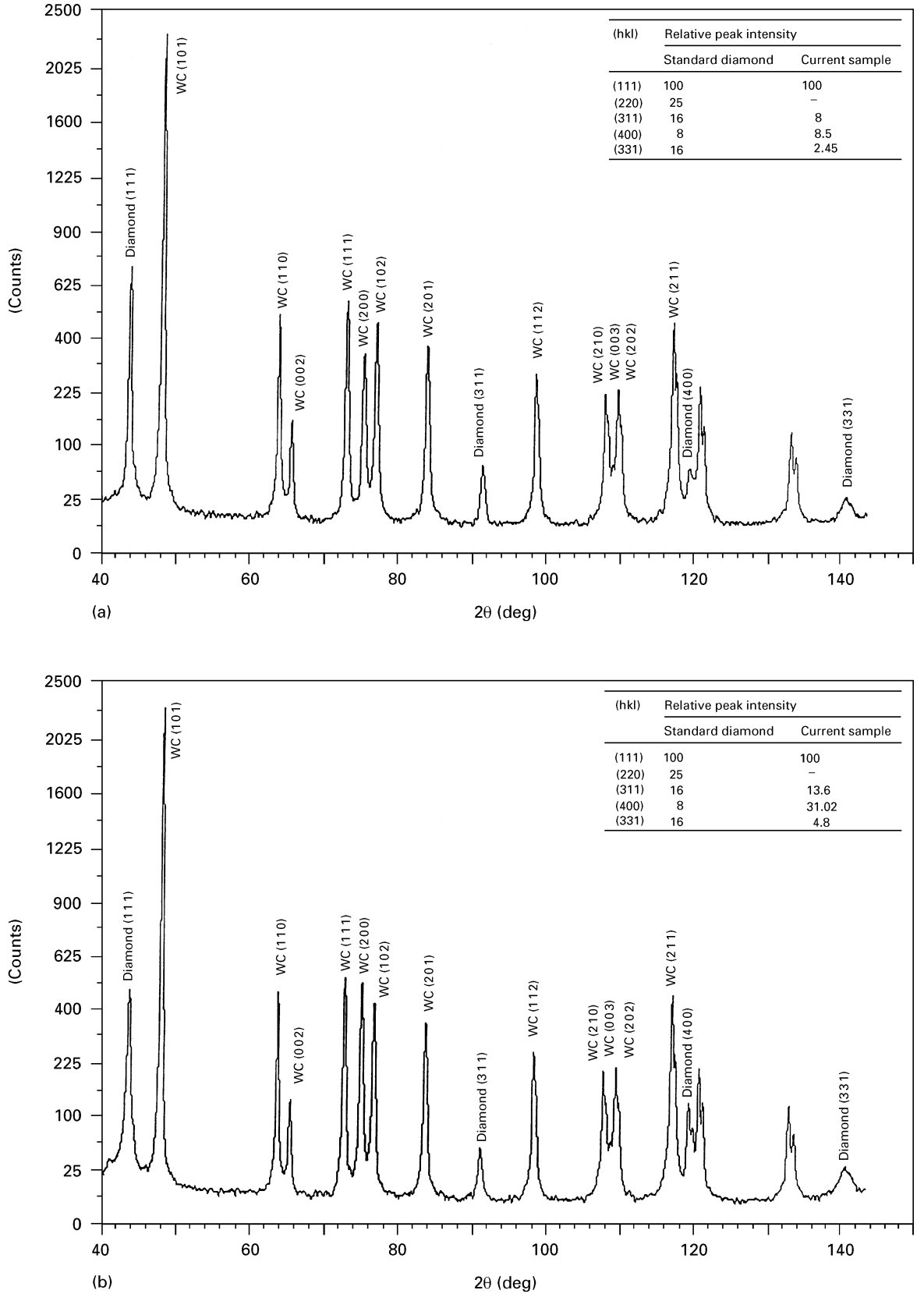

Figure 6 X-ray diffraction spectra for diamond coatings deposited at (a) 1, (b) 3, (c) 5, (d) 7, and (e) 9 vol % methane, respectively.

peak intensity of the deposited films to that of standard randomly oriented diamond are given in the table attached to each spectrum. All the XRD spectra showed the presence of reflections from the WC substrate planes. The purpose of generating the XRD plots was to determine the preferred orientation or texture of the samples at different methane concentrations. A comparative figure was obtained by comparing the relative peak intensities of all the (*hkl*) reflections with the random intensities from the standard randomly oriented diamond card.

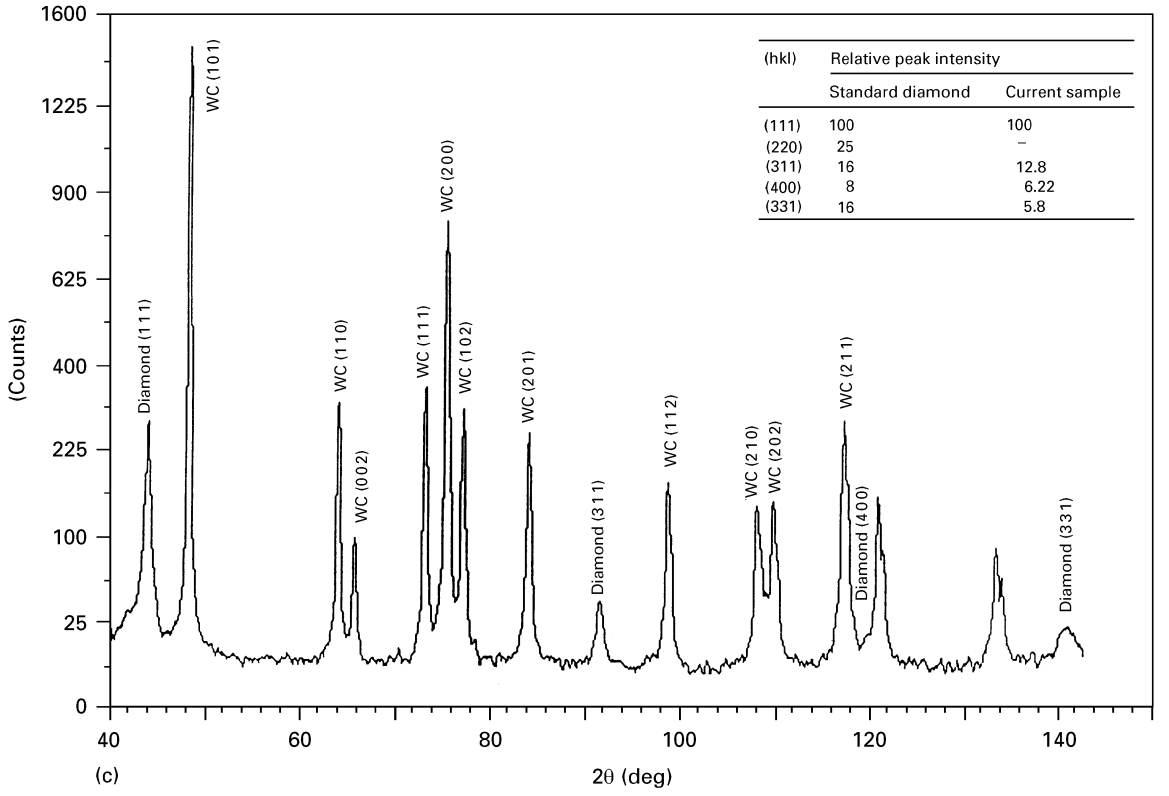

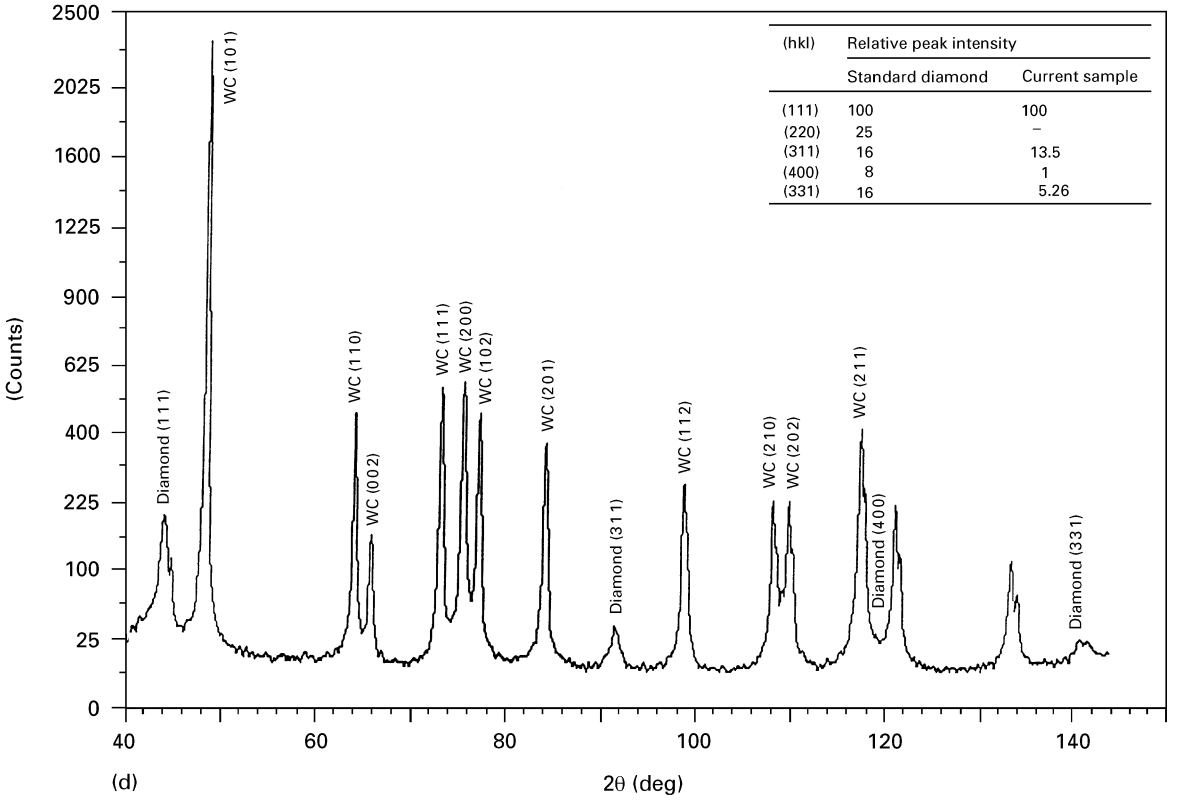

Figure 6 (continued)

To perform the comparison, the texture coefficient [23] was calculated for each sample as follows:

$$T^*_{h'k'l'} = \frac{I_{h'k'l'}}{I^0_{h'k'l'}} \Big/ \frac{1}{n}\sum_0^n \frac{I_{hkl}}{I^0_{hkl}} \quad (1)$$

where $T^*_{h'k'l'}$ is the texture coefficient for the reflection (hkl) and $I^0_{h'k'l'}$ is the standard random peak intensity for the reflection (hkl). The term $(1/n \sum_0^n (I_{hkl}/I^0_{hkl})$ represents the average overall observed (hkl) reflections of the ratio of measured to standard peak intensity values. The diamond reflection (220) at $2\theta = 75.304^\circ$ was difficult to detect due to the presence of a tungsten carbide (200) peak from the substrate at $2\theta = 75.445^\circ$. Therefore, only the remaining four

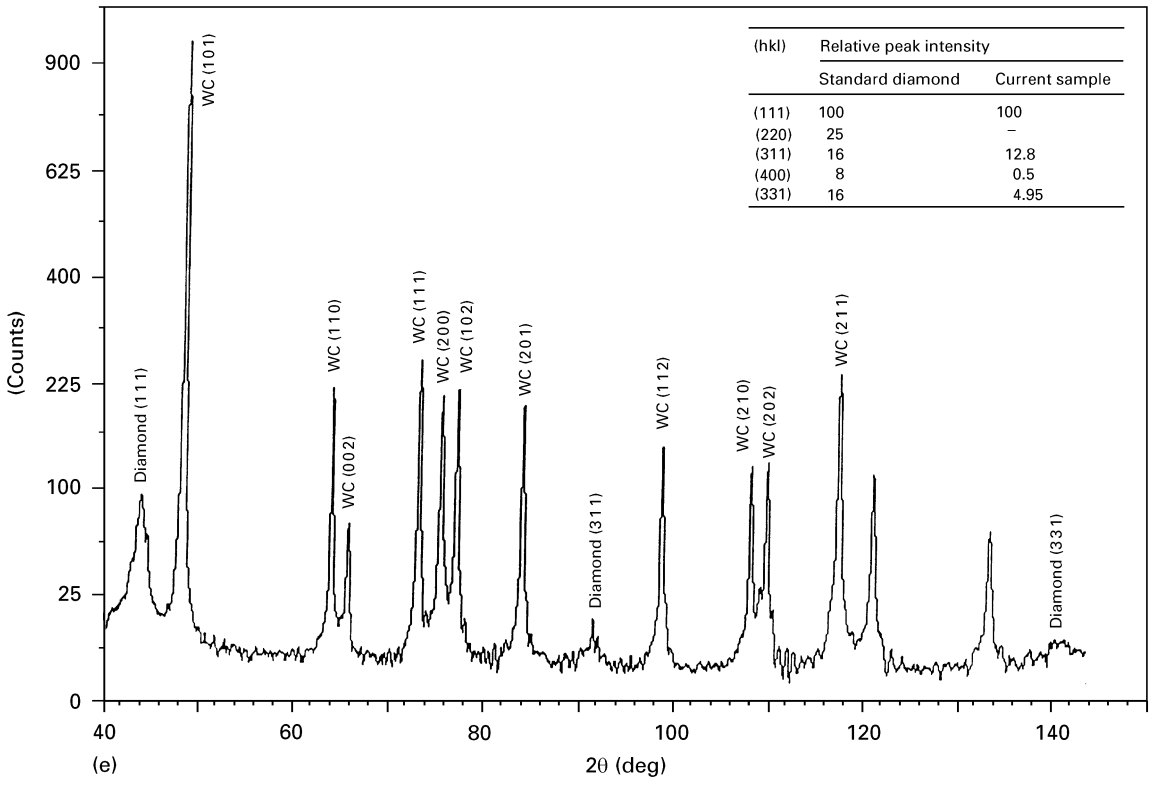

Figure 6 (continued)

reflections of diamond, (111), (311), (400) and (331), were examined.

Fig. 7 is a plot of the texture coefficient versus the methane concentration. According to the plot, it is evident that the diamond film tends to grow with a (400) texture at the expense of the other three orientations, especially the (111) orientation up to a 3 vol % methane concentration. Here, the (400) texture reaches an optimum value and then declines severely while the other orientations increase steadily. For methane concentrations higher than 3 vol %, (111) becomes the dominant orientation. However, the peak intensities of all the diamond crystallographic planes become weaker than WC peak intensities as a result of a decrease in the diamond phase.

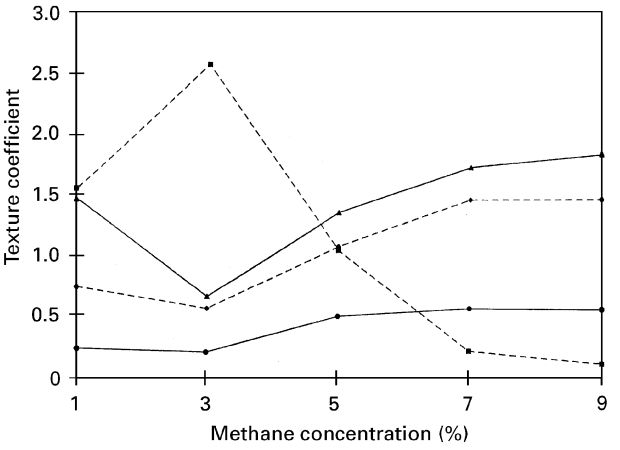

Figure 7 The texture coefficient versus the methane concentration (-▲-), (1 1 1); (- ◆ -), (3 1 1); (- ■ -), (4 0 0); (-●-), (3 3 1).

3.5. Chemical quality

The chemical quality of diamond-coated inserts was analysed utilizing Raman spectroscopy. The two objectives of the Raman analysis were to determine the effect of methane concentration on the chemical quality of the deposited diamond films at the cutting tip, and to examine the chemical uniformity along the surface.

Raman spectra of diamond films deposited on cemented carbides at 1, 3, 5, 7, and 9 vol % methane are shown by Figures 8, a, b, c, d and e, respectively. These spectra were collected at the rake region of the cutting tip of each sample. Fig. 8 curves a and b show a sharp peak at 1336 cm^{-1}, indicating the presence of diamond. The observed shift in the peak position compared with natural diamond can be caused by either a convolution of the microcrystalline domain size and/or a compressive residual stress [24]. The full width at half maximum (FWHM) calculated for each peak is shown next to the peak position. The deviation in the calculated values of FWHM from that of natural diamond can be explained by disordered sp^3-bonded carbon. The broader peak observed at 1553 cm^{-1} can be correlated to the existence of amorphous carbon (a-C) in the grain boundaries of diamond crystals [25]. As anticipated, diamond films deposited at a methane concentration greater than 3 vol % began to show the presence of increased amounts of non-diamond species. As shown in Fig. 8, curve c, an a-C hump is observed at 1560 cm^{-1} combined with a relatively small peak at 1355 cm^{-1} representing pyrolitic graphite which is a disordered form of microcrystalline graphite [25]. A greatly shifted diamond peak is present at 1340 cm^{-1} combined with a weak broad shoulder at 1140 cm^{-1} representing

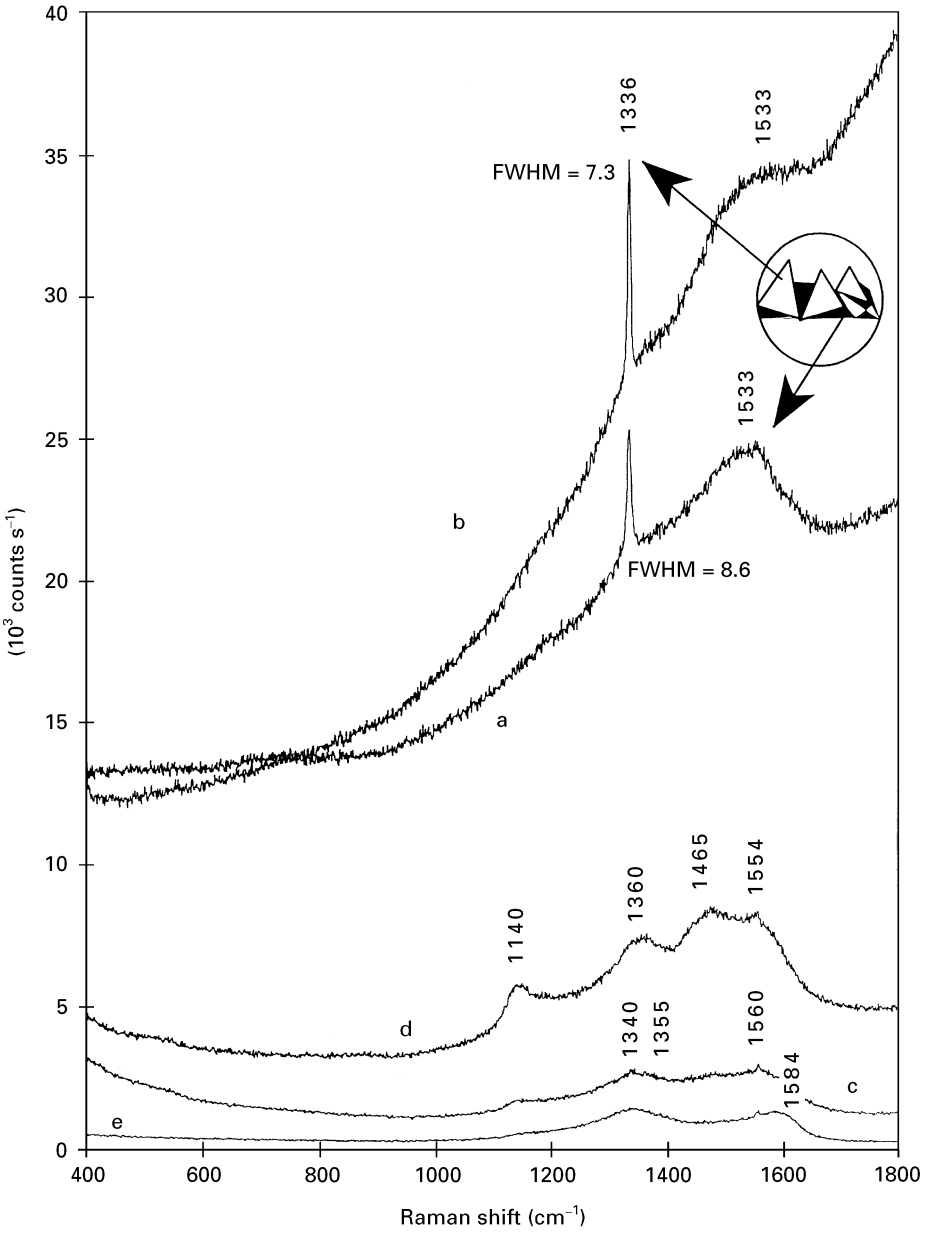

Figure 8 Raman spectra of diamond films deposited on cemented carbide inserts at (a) 1, (b) 3, (c) 5, (d) 7, (e) 9 vol % methane, respectively.

microcrystalline diamond [1]. Similarly, for Fig. 8, curve d, the a–C hump at 1560 cm^{-1} is shifted to 1554 cm^{-1} and the microcrystalline graphite presence becomes stronger at 1360 cm^{-1}. Although the diamond peak greatly faded in this case, it does not mean that diamond is not present. The XRD plot in Fig. 6d for this particular sample indicated that diamond still exists. However, the fading of the diamond peak indicates an increased graphitic content. The contribution of microcrystalline diamond in the spectrum is evident from the peak at 1140 cm^{-1} [1]. An unidentified peak is present, at 1465 cm^{-1}, which might be a resultant peak from the presence of both highly ordered pyrolitic graphite and a–C. For Fig. 8, curve e, a strong peak at 1584 cm^{-1} indicates the formation of a long-range ordered graphite phase.

To determine the chemical uniformity of the diamond coating along the surface area of a coated tool, a scan was performed at the cutting tip, as well as at the centre of each sample. Fig. 9a and b show the Raman spectra collected at the tip and centre respectively, of a diamond-coated tool insert deposited at 3 vol % methane. As observed from both spectra, the chemical quality was relatively uniform along the surface and did not change drastically with slight variations in substrate surface temperature.

3.6. Residual stress

The residual stress measured using the d verses $\sin^2 \psi$ method in all samples was compressive with a minimum value at 1 vol % methane equal to -270.2 MPa and a maximum value at 5 vol % methane equal to -1318.5 MPa. A typical plot for the latter sample is shown in Fig. 10. It was observed that increasing the methane percentage resulted in an increased compressive stress in the diamond films deposited on cemented carbide inserts.

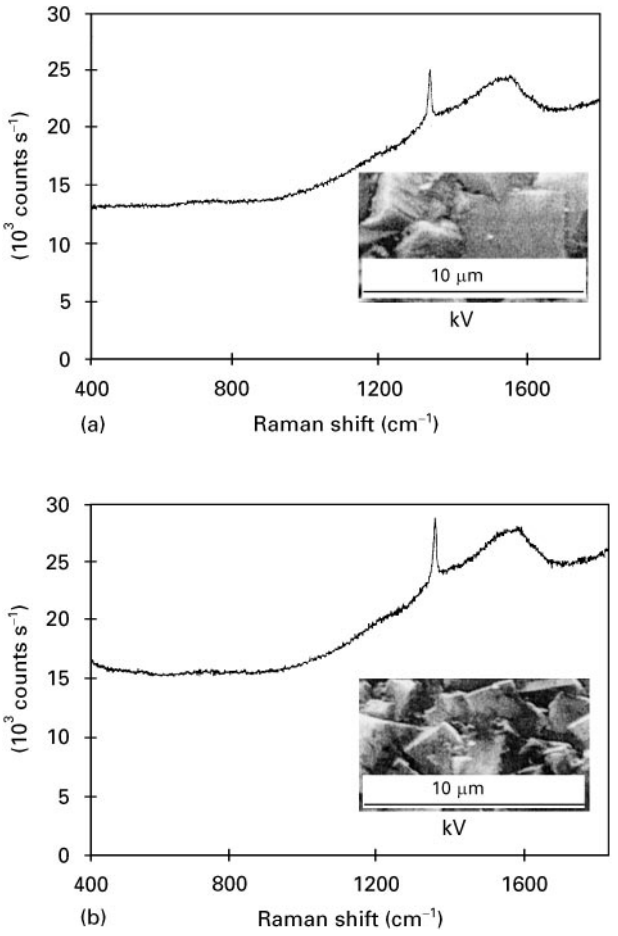

Figure 9 Raman spectra of a diamond-coated tool insert at the cutting tip (a) and at the centre (b).

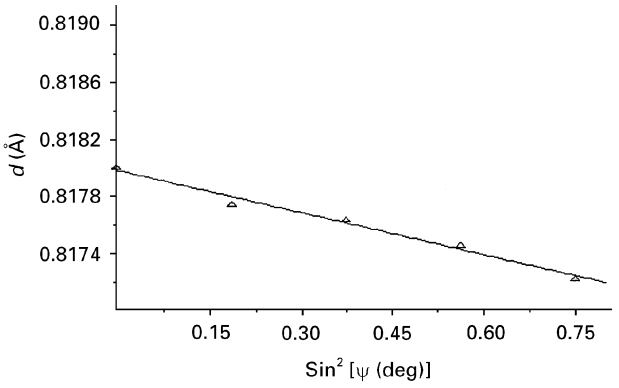

Figure 10 d verses $\sin^2\psi$ plot for residual stress in a diamond-coated tool with diamond deposited at 5 vol % methane (stress, 1006.9 ± 67.8 MPa; $\phi = 0^\circ$). (△), $\psi > 0$.

The increased compressive stress induced by increased methane concentration is a result of increased amounts of impurities such as sp^2-bonded carbon and a–C in the diamond matrix, as revealed from Raman analysis. Windishmann *et al.* [26] proposed an explanation for correlating the induced compressive stress with increased graphite impurities. They observed that graphite which has a large specific volume (1.5 times that of diamond) preferentially nucleated at the grain boundaries of diamond crystallites. In addition, owing to the submicrometre grain structure at high methane percentages, the diamond film possessed a high internal surface area. Therefore, the increased presence of graphite produced a larger compressive stress in the diamond coatings.

4. Conclusions

We have observed that changing the methane concentration greatly affects the physical properties of diamond films deposited using hot-filament CVD on cemented carbide tool inserts. Increasing the methane concentration from 1 to 3 vol % caused a transformation from a (111) orientation to a (100) orientation. For methane concentrations greater than 3 vol % the diamond grains gradually lost their crystalline form and switched to an amorphous-like morphology. The increase in methane concentration also caused a deterioration in chemical quality in the form of an increased presence of non-diamond carbon species. The optimum chemical quality for cutting applications was observed in diamond coatings deposited at 1 and 3 vol % methane. For methane concentrations greater than 3 vol %, the diamond film predominantly consisted of disordered graphite with small traces of diamond. The increased presence of theses non-diamond species resulted in an increase in the residual stress generated in the diamond coatings. The above conclusions were expected to have a great impact on the machining performance of these diamond-coated cemented carbide inserts. Therefore, a continuation of this work was conducted in which the effects of methane variation on several mechanical properties of diamond-coated tool inserts were studied. The results of that work can be found elsewhere [27].

References

1. R. F. DAVIS, "Diamond films and coatings" (Noyes Park Ridge, NJ, 1993).
2. T. H. HUANG, C. T. KUO, C. S. CHANG, C. T. KAO and H. Y. WEN, *Diamond Relat. Mater.* **1** (1992) 594.
3. K. SAIJO, M. YAGI, K. SHIBUKI and S. TAKATSU, *Surf. Coatings Technol.* **47** (1991) 646.
4. *Idem., ibid* **43**–**44** (1990) 30.
5. M. MURAKAWA and S. TAKEUCHI, "Diamond and diamond-like films and coatings" NATO Advanced study Institute Series, Series B: Physics, Vol. 266, edited by R. E. Clausing et al. (Plenum, NewYork, 1991) p. 757.
6. Y. SAITO, T. ISOZAKI, A. MASUDA, K. FUKUMOTO, M. CHOSA, T. ITO, C. E. BAUER, A.INSPECTOR and E. J. OLES, *Diamond Relat. Mater.* **2** (1993) 1391.
7. T. ISOZAKI, Y. SAITO, A. MASUDA, K. FUKUMOTO, M. CHOSA, T. ITO, E. J. OLES, A. INSPECTOR and C. E. BAUER, *Ibid.* **2** (1993) 1159.
8. S. SODERBERG, A. GERENDAS and M. SJÖSTRAND, *Vakuum*, **41** (1990) 1317.
9. I. REINECK, S. SÖDERBERG, K. WESTERGREN and H. SHAHANI, in Proceedings of the Second International Conference on New Diamond Science and Technology, Washington, DC, 1990 (1990).
10. J. OAKES, X. X. PAN, R. HAUBNER and B. LUX, *Surf. Coatings Technol.* **47** (1991) 600.
11. P. M. STEPHAN, R. A. HAY and C. D. DEAN, *Diamond Relat. Mater.* **1** (1992) 710.
12. R. HAUBNER, B. LUX and P. RENARD, *Ibid.* **1** (1992) 1035.
13. D. G. BHAT, D. G. JOHNSON, A. P. MALSHE, H. A. NASEEM, W. D. BROWN, L. W. SCHAPER, and C.-H. SHEN, *Ibid.* **4** (1995) 921.

14. D. G. BHAT, D. G. JOHNSON, and C. E. ZIMMERMAN, paper presented at the ASM Materials Week '93 Symposium on Carbide Cutting Tool Materials, Pittsburgh, PA, October 1993.
15. R. E. CLAUSING, L. HEATHERLY, and E. D. SPECHT, Diamond and Diamond-Like Films and Coatings, edited by R. E. Clausinf et al., Plenum Press, New York, 1991.
16. H. WINDISCHMANN and GLENN F. EPPS, *J. Appl. Phys.* **69 (4)** (1991) 2231.
17. R. HAUBNER, S. OKOLI, and B. LUX, Proceedings of the International Conference on Advances in Hard Materials Production, Bonn, May 4-6, 1992, Paper 44, pp. 1–12.
18. B. LUX and R. HAUBNER, in R. E. Clausing et al. (eds), Diamond and Diamond- like Films and Coatings, NATO-ASI Ser. B: Physics,Vol.226, Plenum, NewYork, 1991, pp. 579–610.
19. H. GUO and M. ALAM, *Thin Solid Films*, **212** (1992) 173.
20. W. ZHU, R. C. MCCUNE, J. E. dEVRIES, M. A. TAMOR, K. Y. SIMON Ng, *Diamond and Relat. Mater.* **4** (1995) 220.
21. M. A. TAHER, Master's thesis, University of Arkansas, Fayetteville, Arkansas, 1995.
22. M.A. TAHER, J. L. SHULTZ, S. NASRAZADANI, H.A. NASEEM, W.D. BROWN, and A.P. MALSHE, Proceedings of the Fourth Int. Syp. on Diamond andDiamond like Materials, Reno, Nevada, May 1995.
23. P. T. MOSELEY, K. R. HYDE, B. A. BELLAMY, and G. TAPPIN, *Corros. Sci.* **24** (1984) 547.
24. M. YOSHIKAWA, G. KATAGIRI, H. ISHIDA, A. ISHITANI, M. ONO, and K. MATSUMURA, *Appl. Phys. Lett.* **55** (25) (1989) 2608.
25. J. ROBERTSON, *Adv. In Phys.* **35** (1986) 317.
26. H. WINDISCHMANN and GLENN F. EPPS, *J of Appl. Phys.* **69 (4)** (1991) 2231.
27. M. A. TAHER, W. F. SCHMIDT, S. NASRAZADANI, H. A. NASEEM, W. D. BROWN, and A. P. MALSHE, *Surf. Coat. Tech.* **86/87** (1996) 678.

Received 18 June 1996
and accepted 17 June 1997